

Edge-on galaxies in the Hubble Ultra Deep Field

V.P. Reshetnikov^{1,2}, P.A. Usachev^{1,2}, S.S. Savchenko^{1,2}

¹ St.Petersburg State University, Universitetskii pr. 28, St.Petersburg, 198504 Russia

² Special Astrophysical Observatory, Russian Academy of Sciences, Nizhnii Arkhyz, 369167 Russia

We studied a sample of 58 edge-on spiral galaxies at redshifts $z \sim 1$ selected in the Hubble Ultra Deep Field. For all galaxies we analyzed the 2D brightness distributions in the V_{606} and i_{775} filters and measured the radial (h_r) and vertical (h_z) exponential scales of the brightness distribution. We obtained evidence that the relative thickness of the disks of distant galaxies, i.e., the ratio of the vertical scale height and radial scale length (h_z/h_r), on average, exceeds the relative thickness of the disks of nearby spiral galaxies. The vertical scale height h_z of the stellar disks of galaxies shows no big changes at $z \leq 1$. The possibility of the evolution of the radial scale length h_r for the brightness distribution with redshift is discussed.

Keywords: galaxies, photometry, evolution

1. Introduction

A study of edge-on spiral galaxies allows a number of important problems of extragalactic astronomy to be investigated: the structure and stability of galactic disks, the properties and distribution of dust in them, the contribution of dark matter to the structure of galaxies, the large-scale distribution of galaxies, etc. (see, e.g., van der Kruit and Searl 1981; Zasov et al. 1991; de Grijs 1998; Mosenkov et al. 2010, 2016; Bizyaev et al. 2017; Makarov et al. 2018; and references therein). The preceding papers were devoted mostly to edge-on galaxies in the local Universe. Only in a few papers the vertical structure of distant objects was studied. For example, Reshetnikov et al. (2003) investigated edge-on galaxies in the Hubble deep fields north (HDF-N) and south (HDF-S). They found that the relative thickness of the stellar disks of galaxies at redshifts $z \sim 1$ exceeds the relative thickness of the disks of nearby galaxies by a factor of 1.5–2. This conclusion was confirmed when analyzing the structure of galaxies in the Hubble Ultra Deep Field (hereafter HUDF) (Elmegreen et al. 2005; B. Elmegreen and D. Elmegreen 2006).

The goal of our paper is a photometric study of edge-on spiral galaxies in the HUDF. The main differences between our paper and the previously pub-

lished studies are: an analysis of the complete two-dimensional (2D) brightness distributions instead of the one-dimensional profiles, using the spectroscopic redshifts for most objects, and a larger size of the sample of edge-on galaxies.

All of the numerical values in our paper are given for the cosmological model with the Hubble constant of $70 \text{ km s}^{-1} \text{ Mpc}^{-1}$ and $\Omega_m = 0.3$, $\Omega_\Lambda = 0.7$.

2. The sample of galaxies and data reduction

To study the edge-on spiral galaxies, we used the HUDF frames in the F606W (hereafter V_{606}) and F775W (i_{775}) filters (Beckwith et al. 2006). In these color bands the HUDF images are deeper than those in other original filters. The pixel size is $0.03''$. In the first step, on the field image in the V_{606} filter we selected 901 galaxies with an apparent flattening $b/a \leq 0.55$, an area ≥ 24 pixels, and $S/N > 3$ in each pixel using the SExtractor package (Bertin and Arnouts 1996). Such a soft constraint on the flattening was used in order not to throw away the galaxies with close neighbors. In several cases, SExtractor does not separate them, but detects them as a single object. Next, based on a visual examination of the images for the objects in different filters and with

different brightness contrasts, we left 77 candidates for edge-on galaxies in the sample.

To analyze the photometric structure (decomposition) of the galaxies, we used the Imfit package (Erwin 2015) with the PSF (point spread function) generated for the HUDF by the Tiny Tim code (Krist et al. 2011). A comparison of the PSF with the sample objects images showed that the disks of all galaxies are resolved with confidence in both radial and vertical directions.

In the selected candidates for edge-on galaxies the bulges are noticeable approximately in a quarter of the objects. In most cases, these bulges are faint and are on the verge of resolution. Therefore, to describe the photometric structure of the galaxies, we chose the simplest model of an edge-on double exponential disk (see, e.g., van der Kriut and Searl 1981):

$$I(r, z) = I_{0,0} \left(\frac{r}{h_r} \right) K_1 \left(\frac{r}{h_r} \right) e^{-z/h_z},$$

where $I_{0,0}$, h_r , and h_z are the central surface brightness, radial and vertical exponential scales of the disk, respectively, and K_1 is a modified first-order Bessel function. The bulges, if they were visible, were fitted by a Sérsic function. The nearby objects projected onto the galaxies under study were masked before the Imfit operation. If, however, the area of the hampering objects was too large, then during the decomposition they were fitted by a combination of different model functions and were subtracted.

An analysis of the residual images (the original image minus the model one) revealed that 19 of the 77 galaxies either are not edge-on galaxies or have a very complex and asymmetric structure. These objects were excluded from the subsequent consideration. Thus, the final sample of edge-on galaxies studied in our paper consists of 58 objects. Examples of our photometric analysis for three galaxies are given in Fig. 1.

For 33 sample galaxies we took their spectroscopic redshifts from Inami et al. (2017) and Rafelski et al. (2015). For 23 objects we used the photometric z from Rafelski et al. (2015) (BPZ redshifts). For two galaxies the redshifts were not found.

The final characteristics of the candidates for edge-on galaxies in the HUDF are listed in Table 1. Column 1 in the table gives the object ordinal number in the sample, columns 2 and 3 provide the coordinates of the galactic center on the original HUDF image in pixels, the next columns give the galaxy number from Coe et al. (2006) and its apparent F606W magnitude

in the AB system of magnitudes (Rafelski et al. 2015). Column 6 gives the redshifts, with the photometric z being marked by colons. For galaxy N47 the photometric z is very low (0.04). This value leads to implausible characteristics of the galaxy and, therefore, we do not use it in the subsequent analysis. Columns 7 and 8 in Table 1 provide the classes introduced by us, which reflect the subjective probability that a galaxy belongs to edge-on ones (*eon*) and the quality of the photometric decomposition (*fit*) (1 means the highest probability and quality, 3 means a low one).

The decomposition results are summarized in the last columns of the table. (We are interested in the scales of the brightness distribution h_r and h_z , so that the central surface brightnesses of the galaxies are not discussed in the paper.) For both exponential scales the first and second numbers refer to the V_{606} and i_{775} filters, respectively. For three galaxies (N1, N15, and N47) the results in Table 1 are presented in arcseconds. The typical measurement error of the scales yielded by the Imfit code is less than 10%.

3. Results and discussion

3.1. General characteristics of the sample galaxies

Figure 2 shows the distributions of the galaxies by the redshift and apparent V_{606} magnitude. The mean redshift of the galaxies we consider is $\langle z \rangle = 1.23 \pm 0.69$ (here and below, the unbiased sample variance is given as an error). The galaxies with spectroscopic z are, on average, nearer than the objects with photometric estimates ($\langle z \rangle = 1.01 \pm 0.34$ vs. $\langle z \rangle = 1.57 \pm 0.92$) and are brighter (Fig. 2).

For the cosmological model adopted in this paper the redshift $z = 1.2$ corresponds to the time elapsed after the beginning of cosmological expansion, ~ 5 Gyr. Consequently, the epochs at which we study the galaxies in the HUDF and the regions of the nearby Universe ($z \approx 0$) are spaced more than 8 Gyr apart. It is hoped that on such a long time scale we will be able to find evidence for the evolution of the global structure of disk galaxies.

Figure 3 shows the distribution of the galaxies at $z \leq 2$ in luminosity. The redshift constraint was used, because the photometric z (only these are known for galaxies at $z > 2$) for distant galaxies are generally less accurate than those for nearer ones. To find the absolute B magnitudes ($M(B)$), we used the results by Sirianni et al. (2005) and for all objects applied the k -correction for an Sc galaxy from Bicker et al.

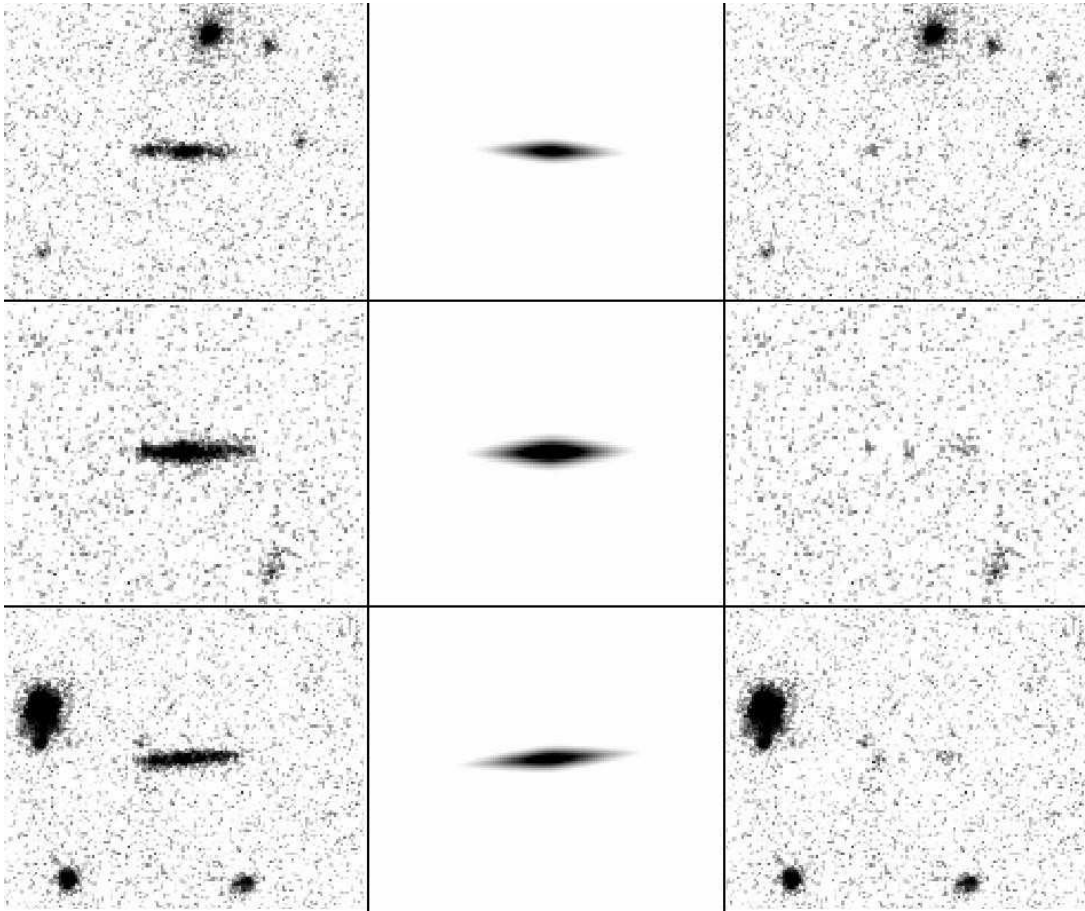


Fig. 1. Examples of photometric modeling for three sample galaxies. From left to right: the original image, the model, and the difference of the original and model images. The upper, middle, and lower rows show, respectively, the images of galaxies N 9 (the frame size along the horizontal axis is $4.6''$), N 22 (the corresponding size is $3.8''$), and N 27 ($4.6''$) from Table 1.

(2004). The mean observed luminosity for the edge-on galaxies in the HUDF is $\langle M(B) \rangle = -18.^m5 \pm 1.^m4$. Given the correction for internal absorption, which reaches $\sim 1^m - 1.^m5$ for edge-on galaxies (see, e.g., Tully et al. 1998), the luminosities of these galaxies seen face-on, on average, reach values in the range from -19^m to -20^m .

Figure 4 shows the distributions of the sample galaxies by h_r and h_z values expressed in kpc in the i_{775} filter. The mean values of these distributions are $\langle h_r \rangle = 1.97 \pm 0.92$ kpc and $\langle h_z \rangle = 0.49 \pm 0.16$ kpc. If we restrict ourselves only to the objects of *eon* and *fit* classes 1 and 2 (the number of such galaxies in the sample is 22), then $\langle h_r \rangle = 2.39 \pm 0.89$ kpc and $\langle h_z \rangle = 0.52 \pm 0.20$ kpc. The above scales look typical for edge-on nearby galaxies (Bizyaev et al. 2014).

The mean ratio of the radial scale lengths in the V_{606} and i_{775} bands is 1.08 ± 0.08 , implying the existence of a color gradient – the stellar disks of distant galaxies are, on average, bluer to the periphery. This

feature is typical for the disks of nearby spiral galaxies. The ratio of the vertical scale lengths in the same filters exhibits no noticeable wavelength dependence: $\langle h_z(V_{606})/h_z(i_{775}) \rangle = 0.97 \pm 0.07$. This is also consistent with the data for nearby galaxies (see, e.g., Bizyaev et al. 2014).

3.2. Sample completeness

Obviously, our sample of edge-on galaxies in the HUDF is incomplete. This incompleteness should be most pronounced for faint and poorly resolvable galaxies, in which the orientation of the stellar disks with respect to the line of sight is difficult to determine.

We will use two methods to roughly estimate the expected number of edge-on galaxies in the HUDF.

On the one hand, consider the general statistics of galaxies in the HUDF. According to Coe et al. (2006), there are ~ 8000 galaxies in this field. The to-

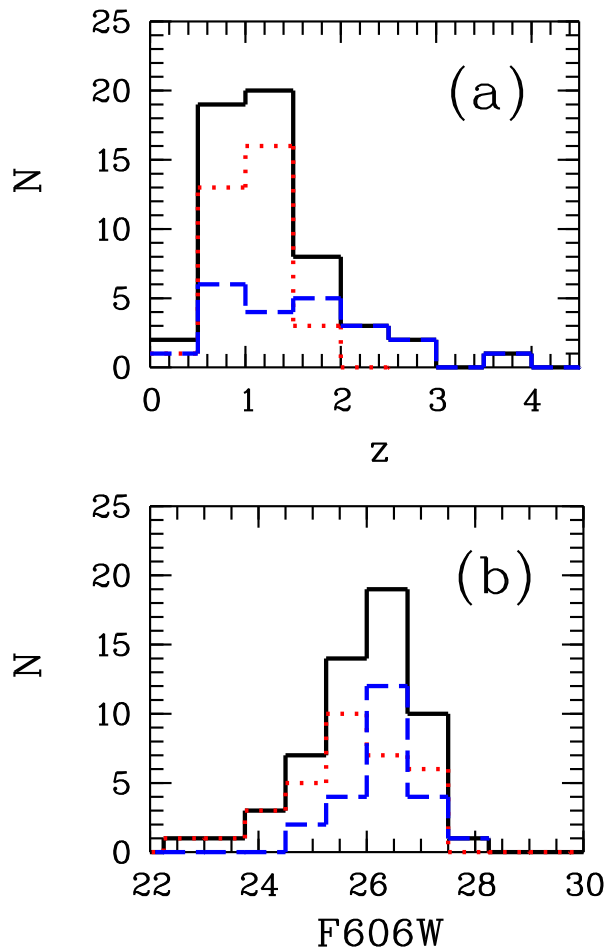


Fig. 2. (a) Distribution of the sample galaxies in redshifts (the dotted (red) and dashed (blue) lines indicate the distribution of the galaxies with spectroscopic and photometric z , respectively; the solid line indicates the combined distribution); (b) the same for the apparent V_{606} magnitudes.

tal number of spiral galaxies selected by their spectral energy distribution with an apparent F606W magnitude brighter than 27.^m5 (this corresponds to the faintest galaxy in our sample) and $z \leq 2$ is 1233. Assuming a random orientation of the galactic planes, we can roughly estimate the relative fraction of edge-on galaxies (with an inclination between the line of sight and the normal to the disk plane $\geq 85^\circ$) to be $|\cos 90^\circ - \cos 85^\circ| = 0.087$. Consequently, the expected number of edge-on spiral galaxies in the HUDF is $1233 \times 0.087 \approx 10^2$.

On the other hand, we can take the luminosity function of nearby edge-on spiral galaxies and estimate how many such objects should be observed toward the HUDF. For our estimation we took the luminosity function of spiral galaxies based on data

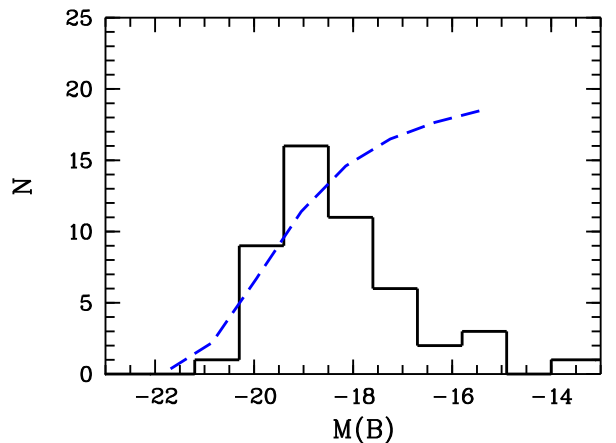


Fig. 3. Distribution of the edge-on galaxies in the HUDF at $z \leq 2$ in absolute B magnitude (solid line). The blue dashed line indicates the expected distribution for edge-on spiral galaxies (see the text).

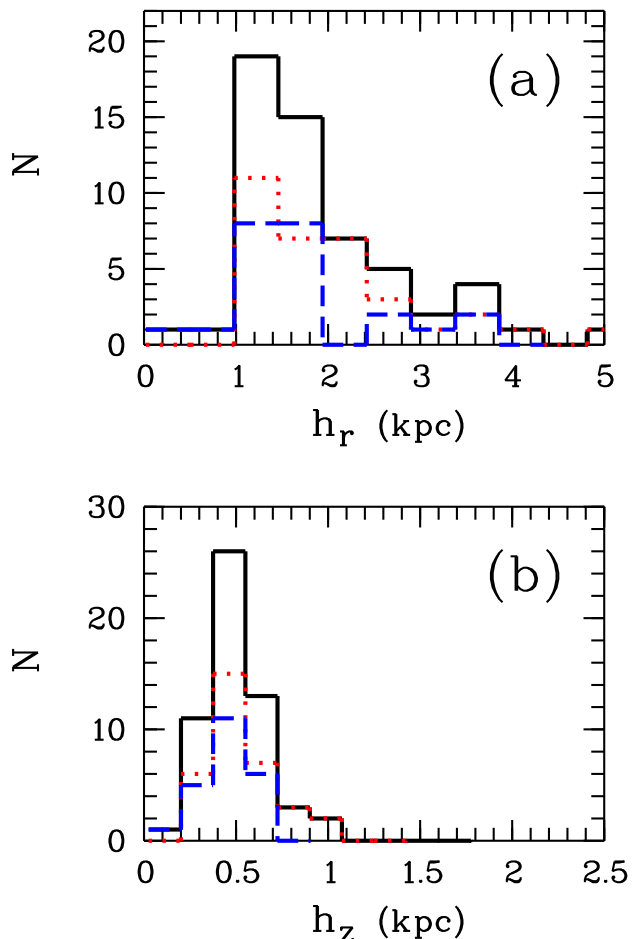


Fig. 4. Distributions of the sample galaxies in (a) radial and (b) vertical disk scales (in kpc). The scales are given in the i_{775} filter. Different lines correspond to different subsamples of galaxies (see the caption to Fig. 2).

from the 2dF survey (Kroton et al. 2005). According to Kroton et al. (2005), the total space density of local spiral galaxies in the range of absolute magnitudes from $M(B) = -15^m$ to $M(B) = -21^m$ (Fig. 3) is 0.022 Mpc^{-3} . Consequently, the space density of edge-on galaxies is $0.022 \times 0.087 = 0.002 \text{ Mpc}^{-3}$. Having integrated this space density towards the HUDF (its angular size is $\sim 10^{-6}$ sr), we found that within $z \leq 2$ about 90 galaxies should be observed in the field. The expected distribution of these 90 galaxies in luminosity is indicated in Fig. 2 by the blue dashed line.

It can be seen from Fig. 3 that for bright (with $M(B) \leq -18^m$) objects the number of galaxies selected in the HUDF roughly agrees with the expected one. The observational selection for fainter galaxies is apparently much stronger. Consequently, for bright galaxies our sample is probably relatively complete, while many galaxies can be missed among the fainter objects.

It is worth noting that the above reasoning is not too reliable, because in Fig. 3 we compare the observed luminosities of distant edge-on galaxies with the luminosities of nearby galaxies. Because of their edge-on orientation, the distant galaxies look fainter by $\sim 1^m$ than the face-on galaxies. On the other hand, however, the galaxies at $z \sim 1$ should be brighter than the nearby objects approximately by 1^m due to the evolution of their luminosity. Both effects can partly compensate each other out and, therefore, for illustrative purposes we still compare the luminosities of the nearby and distant galaxies in Fig. 3.

Another factor that is difficult to take into account is the evolution of the properties of the spiral galaxies themselves. Because of this effect, many of the distant galaxies that look irregular and asymmetric at $z \sim 1$ can evolve into typical spiral galaxies with thin stellar disks by $z \sim 0$.

3.3. Relative thickness of the stellar disks

The mean ratio of the radial and vertical exponential disk scales for the entire sample (58 galaxies) in the i_{775} band is $\langle h_r/h_z \rangle = 4.02 \pm 1.28$. If we restrict ourselves only to the objects of classes 1 and 2, which characterize the probability of assignment to edge-on galaxies and the decomposition quality, then $\langle h_r/h_z \rangle = 4.61 \pm 0.98$ (22 galaxies). In the V_{606} filter the corresponding quantities are $\langle h_r/h_z \rangle = 4.46 \pm 1.45$ and $\langle h_r/h_z \rangle = 5.27 \pm 1.23$.

These mean values look smaller (i.e., the galactic disks are thicker) than those for spiral galaxies in the nearby Universe. For example, in the biggest present-day catalog of edge-on galaxies containing more than 5000 objects (Bizyaev et al. 2014), the mean values of this ratio vary from 6.34 in i to 7.14 in g (here we took into account the fact that $h_z = z_0/2$; g and i are the SDSS¹ filters). Other samples of edge-on galaxies also suggest thinner stellar disks of nearby spiral galaxies: for example, 7.4 ± 2.6 (the I filter; de Grijs 1998), 16 ± 4 (Sc/Sd galaxies in the R filter; Schwarzkopf and Dettmar 2000), 7.3 ± 2.2 (I ; Kregel et al. 2002), 9.6 (K ; Bizyaev and Mitronova 2002), 7.1 (J ; Mosenkov et al. 2010), 8.26 ± 3.44 (De Geyter et al. 2014), and 8.81 ± 2.78 (Peters et al. 2017). In the last two papers the relative disk thicknesses were obtained by simultaneously modeling the galaxies in the SDSS g , r , i , and z filters. Kregel et al. (2002), De Geyter et al. (2014), and Peters et al. (2017) used the same photometric model as that in our paper to describe the structure of the galaxies. The data from the remaining papers were recalculated by taking into account the ratio $h_z = z_0/2$.

Note that we compare the observed relative thicknesses of the galaxies from the HUDF with those for the nearby edge-on galaxies. This is because the stellar disks seen edge-on look more extended due to the integration of emission along the line of sight. This effect can introduce certain systematics into the radial scale lengths measured by different methods. For example, Padilla and Strauss (2008) and Rodriguez and Padilla (2013) estimated the thickness of spiral galaxies by studying the distribution of galaxies from SDSS in apparent flattening. As the apparent flattening these authors took the SDSS axial ratio found by fitting the galaxies with an exponential model. According to the first and second papers, the true flattening of the disks of spiral galaxies is 0.21 ± 0.02 and 0.27 ± 0.009 , respectively. These values correspond to $h_r/h_z = 4.8$ and 3.7 are close to our data for distant galaxies. On the other hand, detailed modeling of the structure of nearby edge-on galaxies is in conflict with such large stellar disk thicknesses (see the references above).

Figure 5 shows the positions of our edge-on galaxies with *eon* and *fit* classes equal to 1 and 2 on the absolute magnitude – h_r/h_z plane in the i_{775} band. The same figure displays the data from the catalog of nearby edge-on galaxies (Bizyaev et al. 2014). The

¹ <http://www.sdss.org>

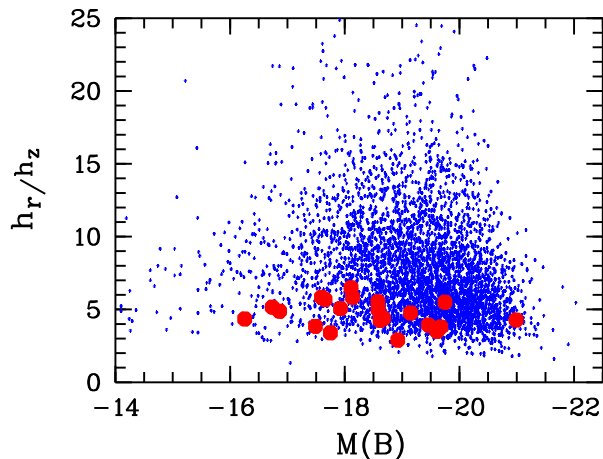


Fig. 5. Distribution of the galaxies from the HUDF on the galaxy absolute magnitude $M(B)$ – radial-to-vertical stellar disk scales ratio plane in the i_{775} filter (red circles). The dots indicate the characteristics of nearby spiral galaxies in the g band from Bizyaev et al. (2014).

galaxies from the HUDF are seen to be located along the lower envelope of the distribution for nearby spiral galaxies, i.e., where there are the thickest observed disks. Thin stellar disks with an exponential scales ratio of ≈ 10 are apparently very rare among the galaxies at $z \approx 1$.

To a first approximation, the reduced ratio h_r/h_z for distant galaxies can be explained by two factors: (1) an increased (in absolute terms) thickness of their disks and (2) shorter disks in the radial direction.

Figure 6 compares the characteristics of the galaxies from the HUDF displayed in Fig. 5 with the parameters of nearby objects on the galaxy absolute magnitude – vertical exponential scale height (in kpc) and absolute magnitude – radial scale length (in kpc) planes.

It can be seen from Fig. 6a that the distant spiral galaxies, though with a large scatter, generally follow the luminosity – stellar disk thickness relation for objects in the nearby Universe. For the radial scale lengths (Fig. 6b) the situation looks differently: the characteristics of relatively faint distant galaxies with $M(B) \geq -18^m$ lie in the same region as that for nearby objects, while brighter galaxies exhibit relatively short stellar disks.

To check this feature, we plotted the characteristics of 49 spiral galaxies at $z = 0.7-1.3$ ($\langle z \rangle = 0.92 \pm 0.14$) from Miller et al. (2011) on the $M(B) - h_r$ plane (the open circles in Fig. 6b). The galaxies from Miller et

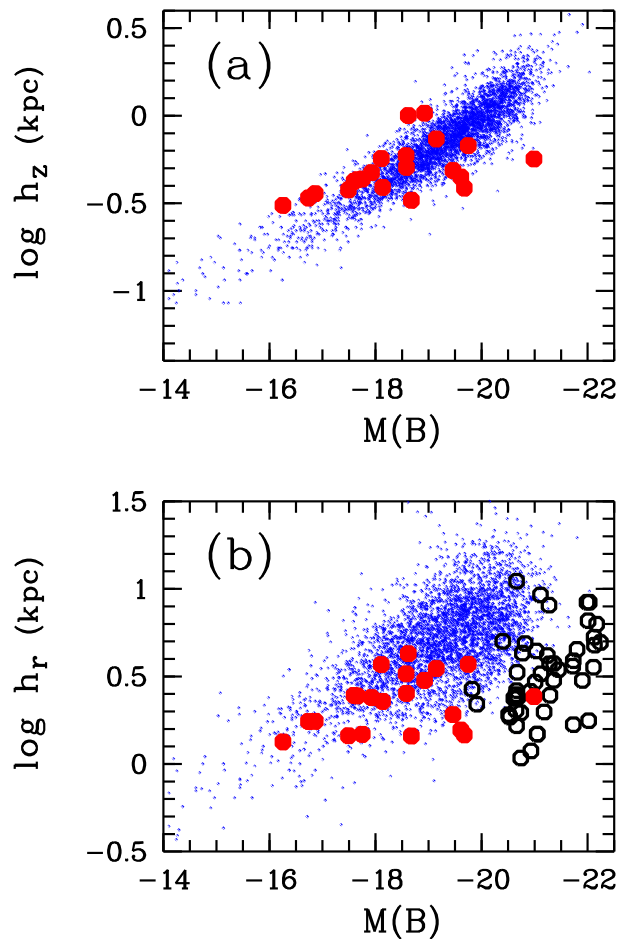


Fig. 6. Distribution of the galaxies from the HUDF (red circles) on the (a) $M(B)$ – disk scale height and (b) $M(B)$ – disk scale length planes. The scales refer to the i_{775} band. The open circles indicate the parameters of distant spiral galaxies from Miller et al. (2011) (z_{850} filter). The dots indicate the characteristics of nearby spiral galaxies in the g band from Bizyaev et al. (2014).

al. (2011) have an arbitrary (not edge-on) orientation and they were selected in the GOODS field of the Hubble Space Telescope. It can be clearly seen from the figure that the distant objects from this paper lie on the $M(B) - h_r$ plane below the nearby galaxies and form a single sequence with the galaxies from the HUDF that deviates from the sequence for the objects at $z \sim 0$. The galaxies from Miller et al. (2011) are, on average, brighter than the objects of our sample (the correction for internal absorption does not compensate for the luminosity difference), so that, on the whole, the results of our papers complement each other.

In Figs. 5 and 6 we compare the observations of distant galaxies in the i_{775} filter with the data for nearby galaxies in the g filter (the effective wavelength of the filter is ≈ 4600 Å). This is not quite correct since, due to cosmological redshift, the observed i_{775} filter at $z \approx 1$ corresponds to wavelength range ≈ 3500 – 4000 Å in the galaxy rest frame. Since the vertical scale height of the stellar disks depends weakly on wavelength (see above), the difference between the color bands plays no major role for them. The exponential scale lengths show a wavelength dependence: the values of h_r , on average, decrease with increasing wavelength. Given this effect, the difference between the distant and nearby galaxies in Figs. 5 and 6 is even more pronounced.

Thus, our results in combination with the data from Miller et al. (2011) may provide evidence for *differential* evolution of the radial sizes of spiral galaxies at $z \leq 1$: the low-luminosity objects show no evidence of evolution, while the bright spiral galaxies from $z \sim 1$ to the present epoch should grow by a factor of 2–3. On the other hand, the scale height of spiral galaxies shows no evidence of noticeable evolution at $z \leq 1$ (Fig. 6a). Consequently, the increased relative thickness of the stellar disks of spiral galaxies at $z \sim 1$ is explained primarily by the smaller radial sizes of their disks.

The results obtained are consistent with the numerical simulations within Λ CDM cosmology. For example, Brook et al. (2006) showed that at $z \sim 1$ the scale heights of the stellar disks are already close to the present-day ones, while the radial scales are noticeably shorter. The quantitative agreement between the results looks good. For example, according to table 2 from Brook et al. (2006), a spiral galaxy at $z \sim 0.9$ with $M(B) = -21.^m1$ (seen edge-on, the galaxy will be fainter approximately by 1^m), $h_r = 2.9$ kpc, and $h_z = 0.63$ kpc will evolve by $z = 0$ into a galaxy with $M(B) = -19.^m7$, $h_r = 4.1$ kpc, and $h_z = 0.65$ kpc. Thus, between $z \sim 0.9$ and the current epoch the relative thickness of the model galaxy changed from $h_r/h_z = 4.6$ to 6.3, with this change having occurred due to the growth of the galaxy in the radial direction.

Based on numerical simulations, Brooks et al. (2011) showed that the evolution of disk galaxies depends on their mass. The massive spiral galaxies at $z \leq 1$ mostly grow in the radial direction; for the low-mass ones the change in their sizes is less pronounced, but, on the other hand, the luminosity changes more dramatically (see table 3 in Brooks et al. (2011)). The

sizes of spiral galaxies increase due to the external accretion of matter and the merging of satellites.

4. Conclusions

Based on an analysis of the HUDF images, we produced a sample of 58 candidates for edge-on spiral galaxies at a mean redshift $z \sim 1$. For all galaxies we analyzed the 2D brightness distributions in the V_{606} and i_{775} filters and determined the radial and vertical exponential scales of the brightness distribution.

Our main results are as follows:

- The scale height of the stellar disks of spiral galaxies shows no significant evolution at $z \leq 1$.
- The relative thickness of the disks of distant galaxies, on average, exceeds the relative thickness of the disks of nearby spiral galaxies. Thin stellar disks at $z \sim 1$ are apparently very rare.
- We obtained evidence for differential evolution of the exponential scale lengths of the stellar disks of galaxies: the bright spiral galaxies at $z \sim 1$ look shortened compared to the nearby objects; the low-luminosity galaxies show no evidence of evolution.

The results of this paper are based on a small sample of galaxies and, undoubtedly, need to be confirmed with a larger number of objects. On the whole, our observational results are consistent with the current views of the evolution of the disk subsystems of galaxies and they can be used to test various models for the evolution of spiral galaxies.

This work was supported by the Russian Science Foundation (grant no. 19-12-00145).

We are grateful to A.V. Mosenkov for useful comments.

REFERENCES

1. S.V.W. Beckwith, M. Stiavelli, A.M. Koekemoer, J.A.R. Caldwell, H.C. Ferguson, R. Hook, R.A. Lucas, L.E. Bergeron, et al., *Astron. J.* 132, 1729 (2006).
2. E. Bertin and S. Arnouts, *Astron. Astrophys. Suppl. Ser.* 117, 393 (1996).
3. J. Bicker, U. Fritze-v. Alvensleben, C.S. Moller, and K. J. Fricke, *Astron. Astrophys.* 413, 37 (2004).
4. D. Bizyaev and S. Mitronova, *Astron. Astrophys.* 389, 795 (2002).
5. D.V. Bizyaev, S.J. Kautsch, A.V. Mosenkov, V.P. Reshetnikov, N.Ya. Sotnikova, N.V. Yablokova, and R. W. Hillyer, *Astrophys. J.* 787, 24 (2014).

6. D.V. Bizyaev, S.J. Kautsch, N.Ya. Sotnikova, V.P. Reshetnikov, and A.V. Mosenkov, *Mon. Not. R. Astron. Soc.* 465, 3784 (2017).
7. Ch.B. Brook, D. Kawata, H. Martel, B.K. Gibson, and J. Bailin, *Astrophys. J.* 639, 126 (2006).
8. A.M. Brooks, A.R. Solomon, F. Governato, J. McCleary, L.A. MacArthur, C.B.A. Brook, P. Jonsson, T.R. Quinn, et al., *Astrophys. J.* 728, 51 (2011).
9. D. Coe, N. Benitez, S.F. Sanchez, M. Jee, R. Bouwens, and H. Ford, *Astron. J.* 132, 926 (2006).
10. D.M. Elmegreen, B.G. Elmegreen, D.S. Rubin, and M.A. Schaffer, *Astrophys. J.* 631, 85 (2005).
11. B.G. Elmegreen and D.M. Elmegreen, *Astrophys. J.* 650, 644 (2006).
12. P. Erwin, *Astrophys. J.* 799, 226 (2015).
13. G. de Geyter, M. Baes, P. Camps, J. Fritz, I. de Looze, Th.M. Hughes, S. Viaene, and G. Gentile, *Mon. Not. R. Astron. Soc.* 441, 869 (2014).
14. R. de Grijs, *Mon. Not. R. Astron. Soc.* 299, 595 (1998).
15. H. Inami, R. Bacon, J. Brinchmann, J. Richard, T. Contini, S. Conseil, S. Hamer, M. Akhlaghi, et al., *Astron. Astrophys.* 608, A2 (2017).
16. M. Kregel, P.C. van der Kruit, and R. de Grijs, *Mon. Not. R. Astron. Soc.* 334, 646 (2002).
17. J.E. Krist, R.N. Hook, and F. Stoehr, *Proc. SPIE* 8127, 81270J (2011).
18. P.C. van der Kruit, and L. Searl, *Astron. Astrophys.* 95, 105 (1981).
19. D.I. Makarov, N.A. Zaitseva, and D.V. Bizyaev, *Mon. Not. R. Astron. Soc.* 479, 3373 (2018).
20. S.H. Miller, K. Bundy, M. Sullivan, R.S. Ellis, and T. Treu, *Astrophys. J.* 741, 115 (2011).
21. A.V. Mosenkov, N.Ya. Sotnikova, and V.P. Reshetnikov, *Mon. Not. R. Astron. Soc.* 401, 559 (2010).
22. A.V. Mosenkov, F. Allaert, M. Baes, S. Bianchi, P. Camps, G. de Geyter, I. de Looze, J. Fritz, et al., *Astron. Astrophys.* 592, A71 (2016).
23. P.C. Peters, G. de Geyter, P.C. van der Kruit, and K.C. Freeman, *Mon. Not. R. Astron. Soc.* 464, 48 (2017).
24. M. Rafelski, H.I. Teplitz, J.P. Gardner, D. Coe, N.A. Bond, A.M. Koekemoer, N. Grogin, P. Kurczynski, et al., *Astron. J.* 150, 31 (2015).
25. V.P. Reshetnikov, R.-J. Dettmar, and F. Combes, *Astron. Astrophys.* 399, 879 (2003).
26. U. Schwarzkopf and R.-J. Dettmar, *Astron. Astrophys.* 361, 451 (2000).
27. M. Sirianni, M.J. Jee, N. Benitez, J.P. Blakeslee, A.R. Martel, G. Meurer, M. Clampin, G. de Marchi, et al., *Publ. Astron. Soc. Pacif.* 117, 1049 (2005).
28. R.B. Tully, M.J. Pierce, J.-Sh. Huang, W. Saunders, M.A.W. Verheijen, and P.L. Witchalls, *Astron. J.* 115, 2264 (1998).
29. A.V. Zasov, D.I. Makarov, and E.A. Mikhailova, *Astron. Lett.* 17, 374 (1991).

Table 1. Edge-on galaxies in the HUDF

N	X	Y	CoeID	V_{606}	z	eon	fit	h_r (kpc)	h_z (kpc)
1	1488	4578				1	3	0.21'' 0.21''	0.03'' 0.03''
2	1744	6169	6870	27.05	1.14	2	1	1.76 1.48	0.40 0.44
3	1812	5234	4907	26.48	2.02:	3	1	1.36 1.31	0.43 0.42
4	1941	4739	3840	26.77	0.59:	3	1	1.40 1.20	0.37 0.37
5	2084	4477	3299	25.51	1.22	2	2	2.11 1.92	0.46 0.49
6	2148	6006	6478	25.81	2.94:	2	2	2.51 2.42	0.60 0.57
7	2697	6387	7022	25.03	1.55	3	3	2.79 2.50	0.81 0.77
8	2701	5920	6278	26.62	0.94	2	2	2.77 2.47	0.41 0.42
9	2738	4401	3315	27.58	0.97:	2	1	1.99 1.75	0.31 0.34
10	3240	3843	2332	26.29	0.52	3	2	1.18 1.08	0.39 0.41
11	3401	2811	1057	24.83	0.74:	1	2	3.66 3.28	0.55 0.59
12	3631	5784	5995	25.04	0.95	3	2	1.22 1.20	0.52 0.52
13	3973	6512	7269	24.23	0.73	1	2	3.50 3.51	0.70 0.74
14	4140	6814	8801	25.78	1.31	3	1	2.37 2.35	0.57 0.60
15	4168	6469				3	1	0.18'' 0.16''	0.05'' 0.04''
16	4186	4249	3097	26.56	2.36:	3	1	1.67 1.59	0.63 0.59
17	4213	3054	1242	26.34	2.02:	2	2	4.04 3.72	0.69 0.68
18	4312	8261	9414	27.25	1.38:	3	1	1.96 1.66	0.44 0.46
19	4362	1468	163	27.43	0.65:	3	1	1.09 1.07	0.22 0.23
20	4462	2075	521	25.93	1.04:	1	2	2.53 2.53	0.48 0.51
21	4673	7460	8259	27.33	0.68	3	1	1.17 1.12	0.31 0.31
22	4675	5841	6143	26.97	1.02	1	1	1.67 1.45	0.33 0.38
23	4780	1333	95	26.21	1.76:	2	2	1.64 1.56	0.43 0.45
24	4833	4000	2652	25.17	0.68	1	2	2.46 2.40	0.46 0.47
25	4837	2673	966	26.43	1.04	2	3	1.56 1.44	0.36 0.38
26	4852	2255	666	25.94	1.16	3	1	1.13 1.02	0.33 0.33
27	4942	4289	3101	27.14	1.37	1	1	2.56 2.28	0.34 0.39
28	5022	8056	9171	26.17	0.68	3	1	1.44 1.27	0.37 0.37
29	5023	8224	9425	26.18	1.79:	2	2	1.65 1.47	0.37 0.39
30	5074	2004	446	25.40	1.10	3	1	1.54 1.57	0.36 0.41
31	5404	5620	5615	25.88	1.10	3	1	2.17 1.59	0.77 0.82
32	5560	7272	8351	26.39	1.75:	3	2	1.56 1.49	0.42 0.44
33	5597	9353	9848	26.53	1.04	3	2	2.29 1.96	0.58 0.58
34	5650	9326	9974	25.12	1.02	2	3	2.46 2.21	0.61 0.62
35	5692	2437	833	26.88	1.55	2	1	1.63 1.45	0.31 0.33
36	5781	7049	8624	25.72	0.83	1	1	4.13 3.70	0.56 0.57
37	5811	5988	6038	24.40	0.67	1	2	4.48 4.27	1.08 1.00
38	5959	3306	1612	26.51	1.76:	3	1	1.38 1.36	0.47 0.45
39	6124	4282	3178	26.21	1.91:	3	2	4.43 3.84	0.73 0.63
40	6178	8569	9807	25.88	0.77	1	2	2.62 2.45	0.39 0.43
41	6416	8780	9834	22.55	0.43	2	2	2.69 3.00	0.77 1.03
42	6462	4440	3418	26.59	3.96:	3	3	1.58 1.89	0.46 0.49
43	6486	6320	6922	25.55	1.26	1	3	5.26 5.29	0.55 0.61
44	6491	7924	9139	25.83	1.84	3	3	1.73 1.58	0.36 0.42
45	6746	7127	8372	23.22	0.53	3	3	2.63 2.41	0.55 0.57
46	6785	2367	735	25.72	1.12:	3	2	1.63 1.30	0.44 0.43
47	6789	5075	4661	26.63	0.04:	2	1	0.16'' 0.15''	0.05'' 0.05''
48	6894	7813	7737	24.39	0.53	3	2	1.39 1.37	0.42 0.45
49	6976	2949	1253	27.44	2.88:	3	1	1.39 1.24	0.42 0.41
50	7079	5197	4835	25.48	1.32	3	2	1.55 1.44	0.58 0.56

Table 1. Edge-on galaxies in the HUDF (cont.)

N	X	Y	CoeID	V_{606}	z	eon	fit	h_r (kpc)	h_z (kpc)
51	7429	5431	5408	26.95	1.42	3	2	1.27 1.27	0.38 0.35
52	7792	4286	3143	25.23	1.10	3	2	2.59 2.14	0.60 0.54
53	7856	3452	1732	25.57	0.66:	3	2	1.62 1.65	0.43 0.46
54	7905	3600	2017	26.53	0.63:	2	1	1.42 1.34	0.31 0.31
55	8020	4758	3871	26.16	0.67	1	2	1.93 1.75	0.35 0.36
56	8614	5763	5898	26.01	1.45:	3	3	1.23 1.24	0.57 0.57
57	8800	4950	4321	26.24	1.10	3	3	1.86 1.74	0.48 0.48
58	9259	5065	4360	24.54	0.14:	3	2	0.82 0.77	0.26 0.27